Rise and fall of ferromagnetism in O-irradiated Al2O3 single crystals

Qiang Li, Juping Xu, Jiandang Liu, Huaijiang Du, and Bangjiao Ye

Citation: Journal of Applied Physics **117**, 233904 (2015); doi: 10.1063/1.4922788
View online: http://dx.doi.org/10.1063/1.4922788
View Table of Contents: http://scitation.aip.org/content/aip/journal/jap/117/23?ver=pdfcov
Published by the AIP Publishing

JOURNAL OF APPLIED PHYSICS 117, 233904 (2015)

Rise and fall of ferromagnetism in O-irradiated Al_2O_3 single crystals

Qiang Li,[1,2] Juping Xu,[1] Jiandang Liu,[1] Huaijiang Du,[1] and Bangjiao Ye[1,a)]
[1]State Key Laboratory of Particle Detection and Electronics, University of Science and Technology of China, Hefei 230026, People's Republic of China
[2]China Spallation Neutron Source, Institute of High Energy Physics, Chinese Academy of Sciences, Dongguan 523803, People's Republic of China

(Received 2 April 2015; accepted 9 June 2015; published online 18 June 2015)

In dilute magnetic semiconductors studies, sapphire was usually used as non-magnetic substrate for films. We observed weak ferromagnetic component in Al_2O_3 single crystal substrate, and excluded the possibility of ferromagnetic contaminations carefully by inductively coupled plasma mass spectrometry and X-ray photoelectron spectroscopy. The ferromagnetism rise and fall during the process of annealing-oxygen irradiation-annealing of the sapphire. The ferromagnetic changes are consistent with Al-vacancy related defects detected by positron annihilation spectroscopy. With first-principle calculations, we confirm that Al-vacancy can introduce magnetic moment for 3 μB in Al_2O_3 crystal and form stable V_{Al}-V_{Al} ferromagnetic coupling at room temperature. © *2015 AIP Publishing LLC*. [http://dx.doi.org/10.1063/1.4922788]

I. INTRODUCTION

In recent years, much interest has been raised in the dilute magnetic semiconductors oxides (DMSO) due to their potential applications as spintronic materials.[1–3] Understanding the origin of ferromagnetism in the DMSs is a crucial issue in this field.[4] Recently, room temperature ferromagnetism (RTFM) has been observed in series of metal oxide films such as ZnO, MgO, TiO_2, etc., while the ferromagnetism was always rather weak and the origin of RTFM was also under debate.[5–9] Sapphire is usually used as non-magnetic substrate for dilute magnetic films in experimental studies, while a research on Co-doped ZnO films observed unexpected ferromagnetic signal from Al_2O_3 crystal wafers.[10] Meanwhile, RTFM has been also reported in some of the nanopowders such as Al_2O_3, MgO, and ZnO, and the ferromagnetism was attributed to universal oxygen vacancies.[11] For instance, Xue *et al*. synthesized Al_2O_3 crystalline particles by sol-gel method, and considered that the ferromagnetism attributed to charged oxygen-vacancies from grain surface.[12] However, another study on series of magnetic substrates observed small amount of γ-Fe_2O_3 impurities on the surface of ferromagnetic sapphire, and the sided polished sample contained a lot of O-vacancies that still show absolute diamagnetism.[13] Also, we noticed a weak ferromagnetic signal on some of the Al_2O_3 crystal wafers when we used them as film substrates, and the ferromagnetism cannot be eliminated by surface cleaning. Thus, detailed research is required to determine the origin of ferromagnetism in this system. On the one hand, substrate influence on magnetic properties should be considered in the further experimental studies of dilute magnetic films. On the other hand, Al_2O_3 substrate is highly resistive. The intrinsic ferromagnetism in Al_2O_3 should be reliable experimental evidence for magnetic mechanism of bound magnetic polaron model.[14]

a)Electronic mail: bjye@ustc.edu.cn. Tel: 86-0551-3607404.

II. EXPERIMENTATION

In this topic, the Al_2O_3 substrate with weak ferromagnetic signal was exactly examined by inductively coupled plasma mass spectrometry (ICP-MS) and X-ray photoelectron spectroscopy (XPS) for detecting the unexpected magnetic impurities. On the other hand, we treated the raw wafer at high temperature up to 1200 °C for 20 min and then oxygen-irradiated for the introduced amount of lattice defects. After that, the wafer was re-annealed for 20 min at 1200 °C to eliminate the inject-induced defects. The oxygen-irradiation was completed using a 100 keV Electro-magnetic Isotope Separator at Shanghai Institute of Applied Physics (SIAP). O-ions at 70 keV were implanted into the polished surface of Al_2O_3 crystals at room temperature to a dose of $1 \times 10^{17}/cm^2$. Before and after each treating step, the magnetic behavior and defective condition in the wafer were determined by vibrating sample magnetometer (VSM) and positron annihilation spectroscopy, respectively. Besides, the first-principles calculations based on density functional theory (DFT) were also employed to verify the experimental results and provide further insight in the origin of ferromagnetism in Al_2O_3 crystals.

III. RESULTS AND DISCUSSION

Figure 1 displays the weak ferromagnetic signal in raw Al_2O_3 substrate. The M-H curve was treated to reduce the influence of diamagnetic background. It can be seen that the coercive field was clearly detected in the M-H curve, and the saturation magnetization (M_S) with mass normalization is only about 6×10^{-5} emu/g, which is relatively much smaller than that of diluted magnetic films deposited on them. However, this signal cannot be removed by any surface cleaning. To make clear whether it is originated from unexpected magnetic impurities, we employed XPS and ICP-MS to detect the trace of some impurities on the surface and on the body of the wafer, and the results are shown in Figures 2(a) and 2(b), respectively.

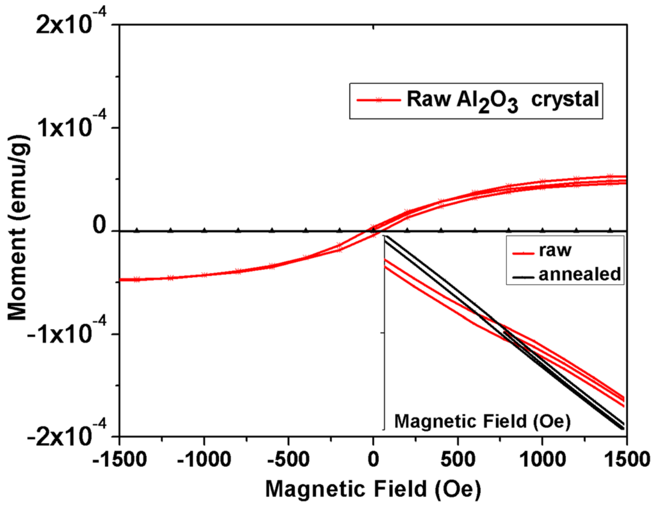

FIG. 1. The room temperature ferromagnetism observed in raw Al_2O_3 crystal substrate. The inset shows virgin measurement results without background subtraction.

As shown in Figure 2(a), the binding energies of Al 2p are located at 74.5 eV, which corresponds to those reported for the core-level XPS spectrum of Al^{3+} ions in Al_2O_3. The O 1s XPS spectra show an asymmetric peak, which can be fitted by two Gaussian curves. The low binding energy peak (red dashes) is located at 531.2 eV for intrinsic binding energy of O^{2+} in Al_2O_3 crystals, and the high binding energy peak (blue dashes) is located at 532.6 eV for probably V_O-related defects or O_2, H_2O, etc., adsorbed on the surface.[15] We have not detected any magnetic impurities on the wafer surface such as Fe, Co, Ni, etc. The XPS spectra measured for Cr element display a broad convex protrusion. The center of protrusion is located at 583 eV, which is close to the binding energy peak of Cr 2p1/2. However, there is no evidence of corresponding Cr 2p3/2 peak observed at 574.3 eV. The 2p peak of Cr^{7+} ions is located at about 580 eV and the binding energy of magnetic Cr-oxides is usually lower than 579.5 eV. This means that we did not observe evidence for magnetic Cr-oxides. Moreover, the spectra spanned over 24 eV are hardly owned to the existence of Cr impurities. The ICP-MS experiment uses Ar ions to bombard internal sample and record the mass spectrum of sample elements, which can detect the trace impurities with an accuracy of 10 ppm. As shown in Figure 2(b), the black lines represent background blank noise, and the red lines are the impurity signals in the wafer. The signal intensity of Al element is 10^7 times larger than that of others (except oxygen), indicating that the impurities are very few. No other magnetic impurities (such as Fe, Co, Ni, Mn, etc.) were detected by ICP-MS experiments, and the results are consistent with the XPS spectra. Meanwhile, we did not observe any signal of Cr element at many of the detected points, indicating no Cr ions exist in the Al_2O_3 wafer. The protrusion in XPS results probably origins from other unexpected factors, or the Cr only exists at a point of surface which is exactly detected by XPS. Actually, the probability of later reason is very little. ICP-MS measurement only showed Pb impurity peak at sample surface with the content of about 20 ppm. Pb is presumably paramagnetic and does not contribute to the ferromagnetic response.

In order to check the ferromagnetism, whether relevant to intrinsic defects in Al_2O_3, we treated this wafer during process of annealing-oxygen irradiation, and then annealing after irradiation. After each treating step, the VSM and slow positron spectroscopy were used to characterize the magnetism and defect structure of sample, and results are shown in Figure 3. Average O-implanted profile simulated by Stopping and Ranges of Ions in Matter (SRIM) program was shown in the inset of Figure 3(a). The irradiated layer was approximately 160 nm in the range of 20–180 nm and the implanted peak of atomic concentrations is about 10 at. % at 106 nm. The red regions represent the content of vacancy type defect caused by irradiation. The vacancies distribute from surface into implanted region, and the profile is different from that of O-ions.

Positron annihilation spectroscopy was proved to be an effective tool for study of vacancy-type defects in materials.[16] Positrons are easily trapped by vacancy defects and

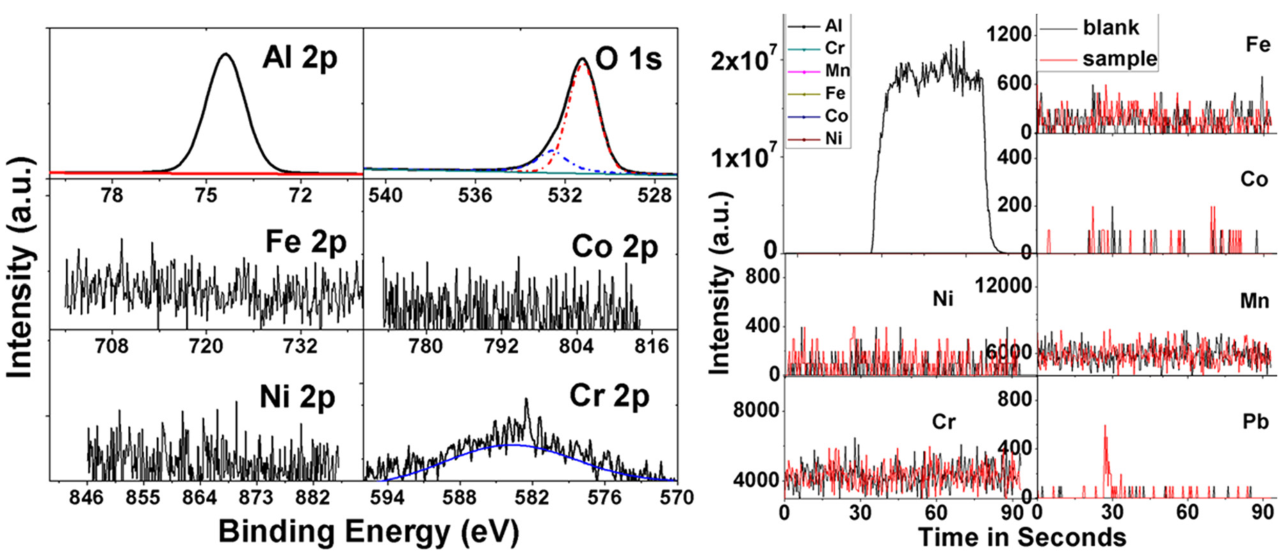

FIG. 2. (a) XPS analysis of the possible impurities on surface of Al_2O_3 substrate; (b) the results of ICP-MS analysis of possible impurities in the wafer.

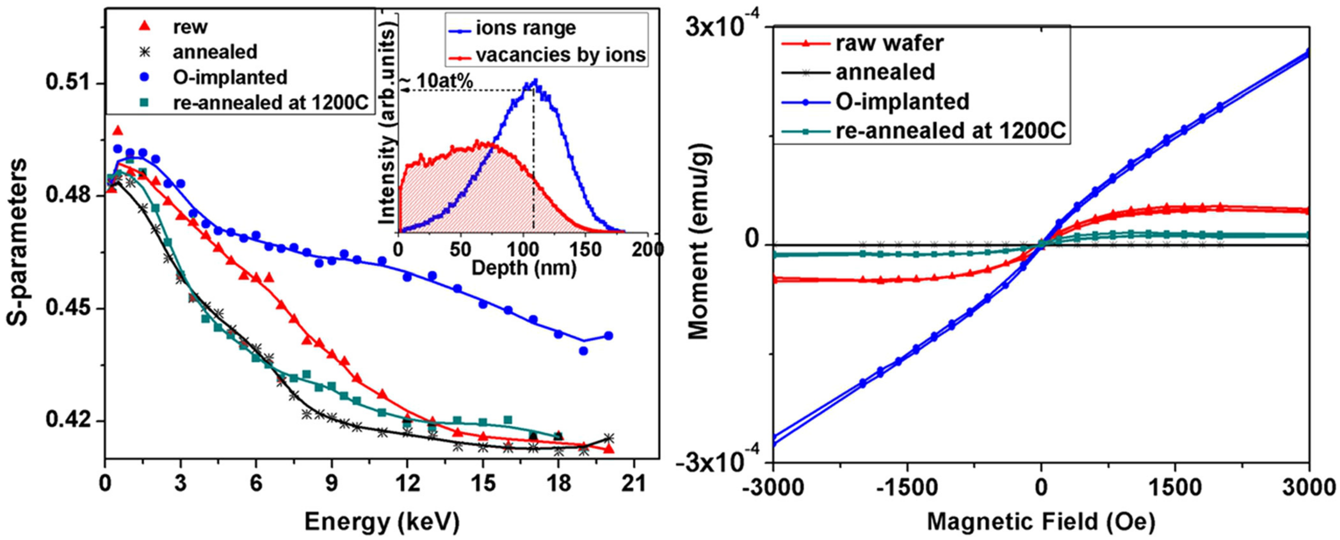

FIG. 3. (a) The S-parameter as a function of positron implantation energy for Al_2O_3 after each treating step. (b) The corresponding changes of M-H curves measured by VSM.

result in a narrowing of 511 keV annihilation peak compared to bulk annihilation. S-parameter was defined as a fraction of counts in the central region of this 511 keV peak.[17] Therefore, positrons annihilated in vacancies will result in an increase in S-parameters. Our experiments were carried out using mono-energetic positron beam with energies ranging from 0.5 to 20 keV. S-parameter as a function of positron implantation energy was used to analyze the V_{Al}-related defects in wafer, and the results are shown in Figure 3(a). Largest S-parameters at the wafer surface are normally due to the formation and annihilation of positronium atoms.[18]

The relatively larger S-parameter in raw wafer when compared with that of after annealing definitely indicates that the raw Al_2O_3 substrate contains amount of positron-trapping potential, which are typically due to Al-vacancies or V_{Al}-related defects. The defects were greatly eliminated after sample annealing at high temperature, since the S-curve significantly decreased. Meanwhile, the ferromagnetism signal almost disappeared, as the M-H curves shown in Figure 3(b). After O-ions irradiation, the significant increase of S-parameters is suitably attributed to formation of V_{Al}-related defects in the sample, and the M-H curves indicate that the sample contains both ferromagnetic and paramagnetic behaviors after irradiation. Furthermore, the implanted sample was retreated at 1200 °C for removing irradiation-induced defects. The value of S-parameters obviously dropped to near the level of initial annealing, and correspondingly the magnetic signal almost disappeared again. Our experimental results definitely indicate that the magnetic performance is consistently following the behavior of V_{Al}-related defects in the sample. At the same time, we excluded the influence of magnetic impurities on observed RTFM by ICP-MS and XPS experiments. Although we did not discuss the action of O-vacancies, the experiments tend to demonstrate that Al-vacancies probably introduce magnetic moment and form ferromagnetic coupling at room temperature in Al_2O_3 substrate as well.

In order to give further insight in Al-vacancy induced RTFM in Al_2O_3 material, a series of first-principle calculations based on DFT were performed using the Vienna *Ab-initio* Simulation Package (VASP).[19,20] The generalized gradient approximation (GGA) method with Perdew-Burke-Ernzerh of (PBE) was employed to describe the exchange correlation energy functional.[21] We built $2 \times 2 \times 1$ Al_2O_3 super-cell with hexagonal structure, which contains 72 O-atoms and 48 Al-atoms for the calculation. The cases of one or two O/Mg vacancies at the center of super-cell were taken into account for discussing magnetic property of vacancy-defects in Al_2O_3 supercell. For the Brillouin-zone sampling, $4 \times 4 \times 4$ Monkhorst-Pack k-mesh was used for the structural optimization and static computation process.[22] The plane wave cut off energy was set to 400 eV, and the relaxed Hellman-Feynman force on each ion was less than 0.01 eV/Å during the optimization. Figure 4 displays the results of total density of electronic states (DOS) for pure and vacancy-defected Al_2O_3 supercell systems. The magnetic moment and polarization energy of the different defected supercell systems are shown in Table I.

DOS patterns of pure Al_2O_3 crystal display no spin polarization emerged around the Fermi energy level which is near the top of the valence band, thus the material shows nonmagnetic property. The band gap between valence band and conduction band is about 6.2 eV, indicating the Al_2O_3 is highly resistive. For the system to contain a neutral O vacancy, it is clear that the V_O does not introduce magnetism in the system, although a negligible impurity band emerges from the bottom of conduction band. We calculated the supercell with a neutral Al vacancy, and found that the top of the valence band shows obvious spin-split, which is crossed by Fermi level. The total magnetic moment value within the Wigner-Seitz radius is about 0.81 μB, as listed in the table. Both the V_O and V_{Al} are not deep level defects in the wide band gap of Al_2O_3 material. The cation vacancies can introduce holes in the oxide system, and electronic compensation

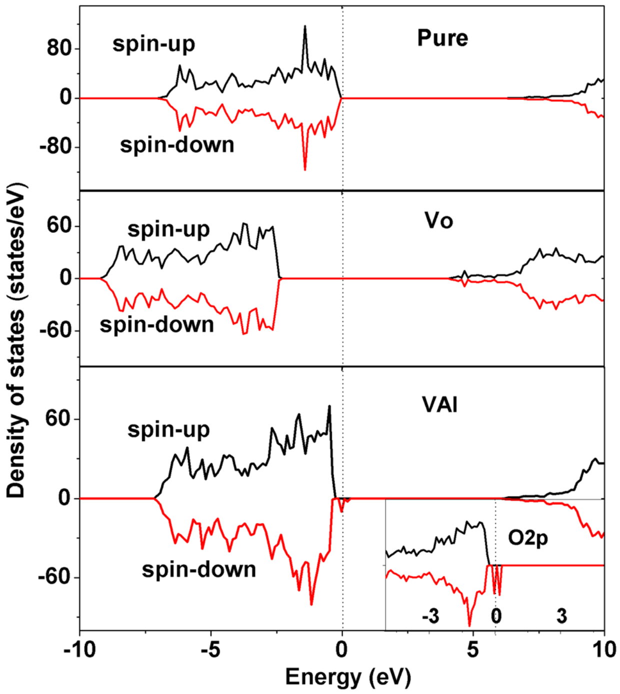

FIG. 4. Total DOS of pure Al_2O_3 and with O/Al vacancies produced by GGA calculation. Inset displays partial DOS of O 2p around Al vacancies in $O_{72}Al_{47}$ supercell.

of 2p electrons from nearby O atoms probably result in redistribution of the energy bands.[23] The inset of Figure 4 displays that splitting impurity bands at Fermi level are mainly caused by the spin-polarization of O2p electrons around Al vacancy, which are the origin of localized moments in the system. Calculated results indicate that the magnetic moments of Al vacancy mostly come from the spin-polarization of O2p electrons. We calculated the total moment of an Al vacancy in static process, and the values are always about 0.81 μB with polarization energy of −281.7 meV, which is defined as the difference of total ground energy between electronic polarized state and non-polarized state. The O2p electrons around Al vacancy show opponent polarized direction with a different polarization degree. We adjusted the polarized direction of O2p electrons and obtained total localized spin of 3 μB with polarization energy about −391.5 meV. This state is more stable than that of initial static process. We consider that the V_{Al} system may have a metastable polarized structure with asymmetric spin direction of O2p electrons. We calculated the magnetic coupling of two Al vacancies in $Al_{46}O_{72}$ supercell with the distance of 0.385 nm, and obtained stable polarization with total moment of 6 μB, as shown in Table I. The energy difference between FM and AFM phases is defined as $\Delta E = E_{AFM} - E_{FM} = 4J_0S^2$, according to Heisenberg model.[24] The J_0 is the nearest-neighbor exchange parameter and S is 3/2. The calculated ΔE is about 46.9 meV, indicating that V_{Al} system has a stable ferromagnetic coupling between the two Al vacancies. Our calculated results are in good agreement with the expectation of experiments.

TABLE I. Magnetic moments (within the Wigner-Seitz radius) introduced by either O or Al vacancies in Al_2O_3 supercell for different defected systems.

System	Pure	V_O	V_{Al} (metastable)	V_{Al} (stable)	V_{Al}-V_{Al}
Polarization energy (meV)	…	0	−281.7	−391.5	46.9 (E_{AFM}-E_{FM})
Magnetic moment (μ_B)	0	0.002	0.81	3.0	6.0

IV. CONCLUSION

In conclusion, we carefully investigated the origin of weak ferromagnetism in Al_2O_3 wafer by using experimental analysis and theoretical calculations. The experimental results indicate that the observed ferromagnetism in experimental Al_2O_3 sample arises from ferromagnetic coupling of Al vacancies instead of magnetic impurities or V_O-related defects. Based on the calculations, the neutral O vacancies are non-magnetic in the Al_2O_3 crystal, while their localized moment is not exactly zero. We have not discussed the possibility of singly charged oxygen vacancies (F^+centers) effect on magnetic performance in our experiments and calculations.

ACKNOWLEDGMENTS

This work was supported by the National Natural Science Foundation of China (Grant Nos. 11175171 and 11475165).

[1]D. Kim, J. Hong, Y. R. Park, and K. J. Kim, J. Phys.: Condens. Matter **21**, 195405 (2009).
[2]Q. Li, B. Ye, Y. Hao, J. Liu, J. Zhang, L. Zhang, W. Kong, H. Weng, and B. Ye, Chem. Phys. Lett. **556**, 237–241 (2013).
[3]K. Rainey, J. Chess, J. Eixenberger, D. A. Tenne, C. B. Hanna, and A. Punnoose, J. Appl. Phys. **115**, 17D727 (2014).
[4]S. A. Wolf, D. D. Awschalom, R. A. Burhman, J. M. Daughton, S. von Molnar, M. L. Roukes, A. Y. Chtchelkanova, and D. M. Treger, Science **294**, 1488 (2001).
[5]M. Khalid, M. Ziese, A. Setzer, P. Esquinazi, M. Lorenz, H. Hochmuth, M. Grundmann, D. Spemann, T. Butz, G. Brauer, W. Anwand, G. Fischer, W. A. Adeagbo, W. Hergert, and A. Ernst, Phys. Rev. B **80**, 035331 (2009).
[6]P. Zhan, W. Wang, C. Liu, Y. Hu, Z. Li, Z. Zhang, P. Zhang, B. Wang, and X. Cao, J. Appl. Phys. **111**, 033501 (2012).
[7]C. Martínez-Boubeta, J. I. Beltrán, Ll. Balcells, Z. Konstantinović, S. Valencia, D. Schmitz, J. Arbiol, S. Estrade, J. Cornil, and B. Martínez, Phys. Rev. B **82**, 024405 (2010).
[8]Ll. Balcells, J. I. Beltrán, C. Martínez-Boubeta, Z. Konstantinović, J. Arbiol, and B. Martínez, Appl. Phys. Lett. **97**, 252503 (2010).
[9]N. H. Hong, J. Sakai, W. Prellier, A. Hassini, A. Ruyter, and F. Gervais, Phys. Rev. B **70**, 195204 (2004).
[10]C. Sudakar, P. Kharel, G. Lawes, R. Suryanarayanan, R. Naik, and V. M. Naik, J. Phys.: Condens. Matter **19**, 026212 (2007).
[11]A. Sundaresan and C. N. R. Rao, Nano Today **4**, 96–106 (2009).
[12]G. Yang, D. Gao, J. Zhang, J. Zhang, Z. Shi, and D. Xue, J. Phys. Chem. C **115**, 16814–16818 (2011).
[13]S. M. M. Yee, D. A. Crandles, and L. V. Goncharova, J. Appl. Phys. **110**, 033906 (2011).
[14]J. M. D. Coey, M. Venkatesan, and C. B. Fitzgerald, Nat. Mater. **4**, 173 (2005).
[15]D. Gao, Z. Zhang, J. Fu, Y. Xu, J. Qi, and D. Xue, J. Appl. Phys. **105**, 113928 (2009).
[16]R. Krause-Rehberg and H. S. Leipner, *Positron Annihilation in Semiconductors, Defect Studies*, Solid-State Sciences Vol. 127 (Springer, Berlin, 1999).
[17]J. Toivonen, T. Hakkarainen, M. Sopanen, H. Lipsanen, J. Oila, and K. Saarinen, Appl. Phys. Lett. **82**, 40 (2003).
[18]B. Y. Zhang *et al.*, Appl. Phys. Lett. **99**, 182503 (2011).

[19]W. Koch and M. C. Holthausen, *A Chemist's Guide to Density Functional Theory* (Wiley, VCH, Weinheim, 2001).
[20]G. Kresse and J. Furthmüller, Phys. Rev. B **54**, 11169 (1996).
[21]J. P. Perdew, K. Burke, and M. Ernzerhof, Phys. Rev. Lett. **77**, 3865 (1996).
[22]H. J. Monkhorst and J. D. Pack, Phys. Rev. B **13**, 5188 (1976).
[23]F. Gao, J. Hua, C. Yang, Y. Zheng, H. Qin, Li. Sun, X. Kong, and M. Jiang, Solid State Commun. **149**, 855–858 (2009).
[24]P. Dev and P. Zhang, Phys. Rev. B **81**, 085207 (2010).